Available online at www.sciencedirect.com

SCIENCE DIRECT®

Diamond and Related Materials 12 (2003) 233–240

DIAMOND AND RELATED MATERIALS

www.elsevier.com/locate/diamond

R&D of diamond films in the Frontier Carbon Technology Project and related topics

Koji Kobashi[a,*], Yoshiki Nishibayashi[a], Yoshihiro Yokota[a], Yutaka Ando[a], Takeshi Tachibana[b], Nobuyuki Kawakami[b], Kazushi Hayashi[b], Kenichi Inoue[b], Kiichi Meguro[c], Hiroshi Imai[c], Hiroshi Furuta[d], Takashi Hirao[d], Kenjiro Oura[e], Yasuhito Gotoh[f], Hironori Nakahara[f], Hiroshi Tsuji[f], Junzo Ishikawa[f], Franz A. Koeck[g], Robert J. Nemanich[g], Tadashi Sakai[h], Naoshi Sakuma[h], Hiroaki Yoshida[i]

[a]*FCT Project/JFCC, Center for Advanced Research Projects, 6F, Osaka University, 2-1 Yamada-oka, Suita, Osaka 565-0871, Japan*
[b]*FCT Project/JFCC, c/o Kobe Steel, Ltd, Electronics Research Laboratory, 1-5-5 Takatsukadai, Nishi-ku, Kobe 651-2271, Japan*
[c]*FCT Project/JFCC, c/o Sumitomo Electric Industries, Ltd, 1-1-1 Koya-kita, Itami 664-0016, Japan*
[d]*Department of Electrical Engineering, Graduate School of Engineering, Osaka University, 2-1 Yamada-oka, Suita, Osaka 565-0871, Japan*
[e]*Department of Electronic Engineering, Graduate School of Engineering, Osaka University, 2-1 Yamada-oka, Suita, Osaka 565-0871, Japan*
[f]*Department of Electronic Science and Engineering, Graduate School of Engineering, Kyoto University, Yoshida-Honmachi, Sakyo-ku, Kyoto 606-8501, Japan*
[g]*Department of Physics, North Carolina State University, Raleigh, NC 27695-8202, USA*
[h]*FCT Project/JFCC, c/o Toshiba Corp., Corporate Research and Development Center, 1, Komukai Toshiba-cho, Saiwai-ku, Kawasaki 212-8582, Japan*
[i]*FCT Project/JFCC, FCT Laboratory, Research Center for Advanced Carbon Materials, National Institute of Advanced Industrial Science and Technology (AIST) Tsukuba Central 5, 1-1-1 Higashi, Tsukuba, Ibaraki 305-8565, Japan*

Abstract

R&D activities on diamond chemical vapor deposition (CVD) and field emission in the Frontier Carbon Technology Project are presented. The topics are (1) morphology control of diamond films grown by a 60-kW, 915-MHz microwave plasma CVD reactor, (2) growth technology of large single crystal diamond with a low density of defects, (3) heteroepitaxial growth technology of diamond films on Pt, (4) fabrication of sharp emitter tips on single crystal diamond, (5) field emission study from diamond particles, and (6) intense field emission from ion implanted homoepitaxial diamond layer. Research results of field emission obtained by Kyoto University and North Carolina State University are also described.

Keywords: Diamond films; Chemical vapor deposition; Etching; Field emission

---

1. Introduction

This article presents selected diamond film research in the Frontier Carbon Technology (FCT) Project: (1) diamond film growth by a 60-kW, 915-MHz microwave plasma chemical vapor deposition (MPCVD) reactor [1–3], (2) growth of large single crystal by CVD [4], (3) heteroepitaxial growth on Pt [5], (4) fabrication of sharp emitter tips [6,7], and (5) fabrication of a field emission device with high current [8]. Our activities mainly aim not at scientific findings but at development of real products and production technologies for the future. Thus, we study on (1) finding CVD conditions for oriented growth, (2) optimization of homoepitaxial growth without noticeable defects, (3) finding optimum conditions for heteroepitaxy on Pt(1 1 1), (4) optimization of diamond microfabrication processes including reactive ion etching (RIE), and (5) optimization of fabrication processes for a high current field emission device. Our emphasis on technological aspects of diamond films, more than on scientific aspects, in this project is based upon our recognition that as production-type large CVD reactors are being developed, application areas of diamond films will be rapidly expanding, and new businesses using diamond films as key com-

---

*Corresponding author. Tel.: +81-6-6879-4146; fax: +81-6-6879-4147.

E-mail address: k-kobashi@rd.kcrl.kobelco.co.jp (K. Kobashi).

0925-9635/03/$ - see front matter © 2002 Elsevier Science B.V. All rights reserved.
doi:10.1016/S0925-9635(02)00298-4

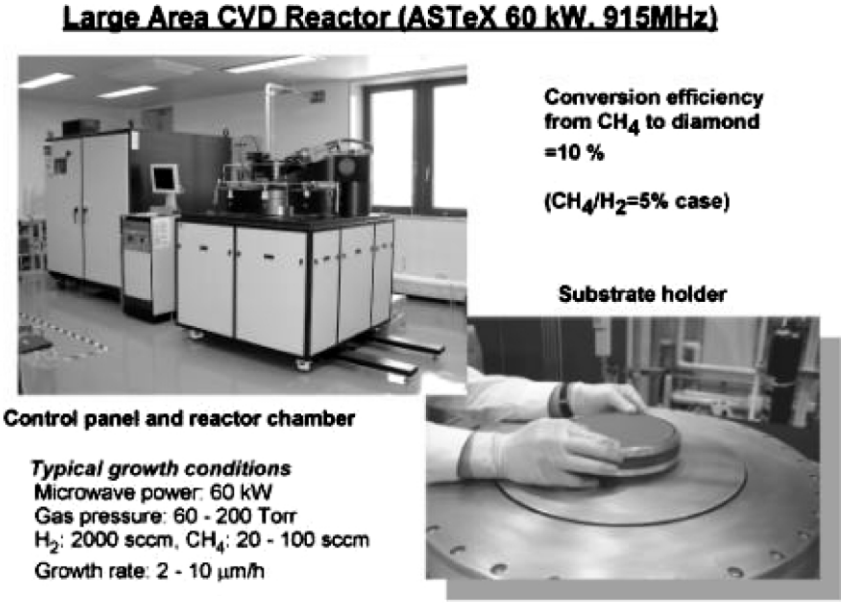

Fig. 1. 60-kW; 915-MHz MPCVD reactor.

ponents are expected to be created in the near future. Regarding scientific aspects, however, we are strongly supported by the members of Osaka University and Prof. Ishikawa's group at Kyoto University on field emission. Also, Prof. Nemanich's group at North Carolina State University undertakes field emission measurements of our specimens using photoemission electron microscopy (PEEM) and field emission electron microscopy (FEEM).

It should be noted that in the FCT Project, diamond film research is also done by Materials Research Laboratory (former NIRIM, n-type doping), Dr Okushi's group (deposition of high quality homoepitaxial layer and study of electronic properties), Prof. Kawarada's group (microfabrication), and Mitsubishi Materials (large area deposition by DC plasma). Our group is closely associated with these groups. In this paper, however, we have to leave them out due to space limitation, but the readers can consult their past and coming references to know the details.

2. Diamond film growth on large area

The purpose of this research is to control diamond film morphologies, using a 60-kW, 915-MHz MPCVD reactor (ASTeX/Seki Technotron), as shown in Fig. 1, by changing the CH_4 concentration c and the substrate temperature T_s that depends on the gas pressure P and the microwave power P_m. Our major interest is to know if there are any differences in α parameters and directions of uniaxial growth between the conventional, 2.45-GHz, quartz-tube-type small reactor that is usually operated under conditions of ($P_m = 300–400$ W, $P = 30$ Torr, $T_s = 700–900$ °C) and the present large reactor that is normally operated under conditions of ($P_m = 60$ kW, $P = 100$ Torr, $T_s = 700–1000$ °C). It might be assumed that given c and T_s, a diamond film with a similar morphology is grown in both cases. It was, however, found that this is not really the case.

Fig. 2 shows the results of α parameters and directions of uniaxial growth obtained by Koidl's group [9] using a quartz-tube-type reactor. This diagram has the following features: (i) the diamond film is $\langle 1\,1\,0 \rangle$-textured for the small c and high T_s region; (ii) as the α-value changes from 1.5 to 3.0, the uniaxial growth orientation changes from $\langle 1\,1\,0 \rangle$ to $\langle 1\,0\,0 \rangle$; and (iii) in the region below $\alpha = 3.0$, the diamond film becomes microcrystalline. In this work, the directions of uniaxial growth were the same as the directions of fastest growth derived from

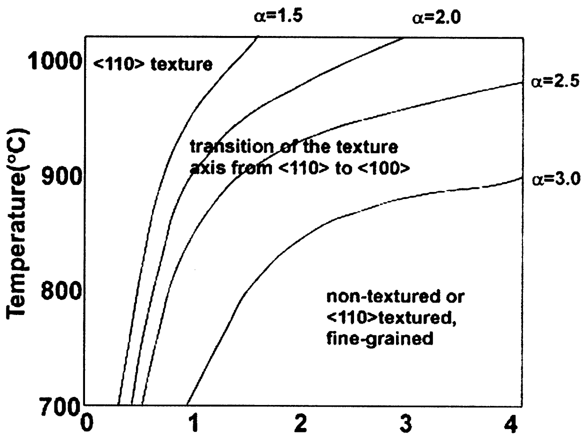

Fig. 2. c–T_s diagram obtained by a 2.45-GHz quartz-tube-type reactor [9].

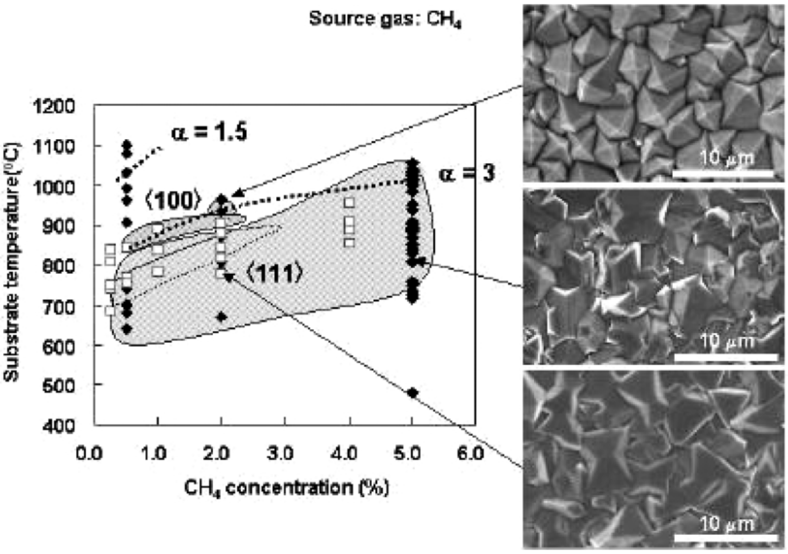

Fig. 3. c–T_s diagram for the large reactor using CH_4 [3]. The ⟨1 1 1⟩ and ⟨1 0 0⟩-oriented domains were determined by X-ray diffraction and the film morphologies were observed by SEM. The rhombus and square points indicate the experimental points.

the shape of CVD diamond crystals, or equivalently α parameters, and this has been considered to be a *basic rule* for α and the direction of uniaxial growth.

In the present work, however, we found [3] that the c–T_s diagram for the large reactor was significantly different from Fig. 2. The c–T_s diagram, when CH_4/H_2 was used as the source gas, is shown in Fig. 3, where we evaluated α and determined uniaxial growth directions by X-ray diffraction. One can see the following differences between Figs. 2 and 3: in Fig. 3, (i) the $\alpha = 1.5$ curve is shifted to the higher T_s side by as much as approximately 200 °C; (ii) similarly, the $\alpha = 3$ curve is shifted to the higher T_s side; (iii) diamond grains with well-defined facets were grown even in the region below the curve of $\alpha = 3$, but only microcrystalline diamond films were grown in Fig. 2; (iv) the diamond films in the region below the $\alpha = 3$ curve have an uniaxial growth direction of ⟨1 1 1⟩, while those in the region immediately above the $\alpha = 3$ curve have an uniaxial direction of ⟨1 0 0⟩. This result seems to show that the directions of uniaxial growth are not directly related with the direction of fastest growth derived from α parameter, or diamond crystal shape. If this is the case, it is in contradiction with the *basic rule* mentioned above. We have repeated growth experiments many times and reproduced the c–T_s diagram of Fig. 3. We do not know yet why such phenomena as (iii) and (iv) occurs in the present case, nor do we understand what governs the phenomena. We can only tell at present that either the high gas pressure or the longer microwave length influences the film morphology. It should be remarkable that in the ⟨1 1 1⟩-oriented film (the bottom photo of Fig. 3), the majority of the diamond faces is (1 1 1) which tend to be directed upwards, and there are many pairs of (1 1 1) faces that are mutually twinned.

To investigate the possibility of growing diamond films with $\alpha < 1.5$, we undertook CVD experiments using $CH_4 + CO_2/H_2$ as a source gas, and the result is shown in Fig. 4. Since both CH_4 and CO_2 can be carbon sources for diamond growth and oxygen generated by decomposition of CO_2 can etch carbon, including diamond, we defined τ in such a way as $\tau = 100\ (c(CH_4) - c(CO_2))/(c(CH_4) - c(CO_2) + c(H_2))$, where $c(X)$ indicates the concentration of X in the source gas. The number associated with each region in Fig. 4 is the α parameter in the region. By comparing Fig. 4 with Fig. 3, one can see the followings: (i) the curve for $\alpha = 1.5$ and 3 are significantly shifted toward the low temperature side; (ii) diamond film growth with $\alpha < 1.5$ is now possible, and indeed, cubic diamond particles with $\alpha \sim 1$ were grown, as seen in the scanning electron micrograph (SEM) at the top of Fig. 4; and (iii) no diamond was formed for $\tau \leqslant 0$ because of etching due to oxygen. Thus, we now conclude that the control of diamond film morphology is possible using CH_4/H_2 or $CH_4 + CO_2/H_2$ as the source gas in the full range of $1 \leqslant \alpha \leqslant 3$ by the large reactor. This achievement is of significance because one can make both highly oriented diamond (HOD) films formed on Si substrate and spontaneously coalesced diamond (SCD) films formed on Pt(1 1 1) thicker in a relatively short time to enhance a coalescence between diamond grains at the film surface, which will lead to single crystal diamond films.

3. Large-area single crystal diamond synthesis by the mosaic method

It is generally recognized that practical applications of diamond, particularly electronic applications, have been hampered by the fact that single crystals with large

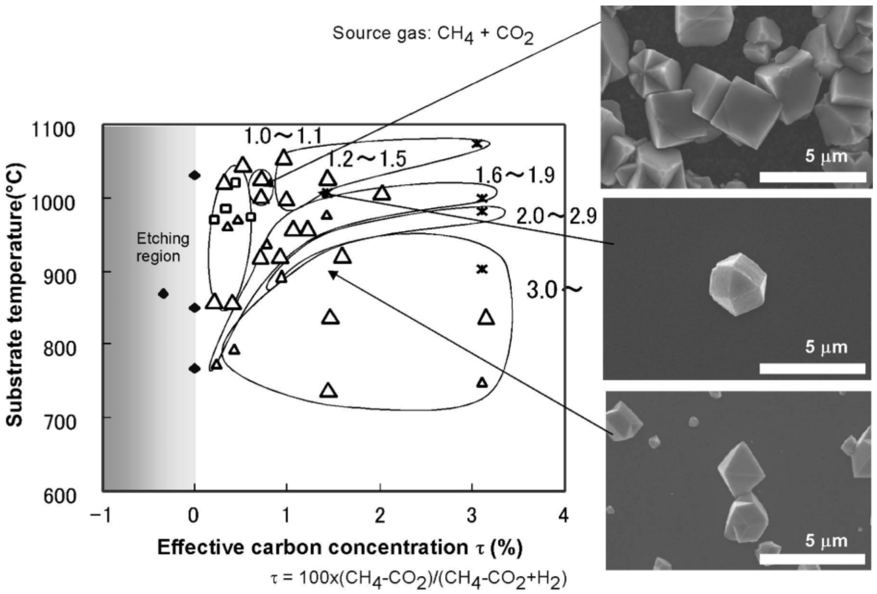

Fig. 4. c–T_s diagram for the large reactor using CH_4+CO_2. The numbers associated with each region is the α parameter. See text for the definition of τ.

surface areas are not commercially available. One of the methods to solve this problem is to homoepitaxially grow diamond by CVD on a diamond mosaic or tile base. Such studies have been done before [10,11] using up to 7 pieces of diamond. In the present study, we used 16 pieces of (1 0 0)-cut Ib diamond of 3×3 and 4×4 mm^2 in size, making the total area 1.44 and 2.56 cm^2, respectively. The most difficult issue of this subject is to deposit diamond by minimizing defects, particularly secondary nucleation due to twin formation. To this end, a 915-MHz, 60-kW CVD reactor was newly designed and constructed with an aid of computer simulations on gas flow and electromagnetic field as well as plasma emission measurements to obtain uniform plasma and temperature distributions across the diamond mosaic. In the latest experiment, using $P_m=40$ kW, $P=100$ Torr, and 5 vol.% CH_4/H_2, a growth rate of 10 μm/h was achieved.

Fig. 5a shows a CVD diamond layer with approximately 8 mm in diameter, which was deposited on a type-Ib diamond (1 0 0) surface of approximately 7 mm in diameter. One can notice that there is no abnormal growth. Fig. 5b shows a mosaic specimen, where a CVD diamond layer of approximately 1 mm thickness was deposited. Although (1 1 1) faces are exposed at the boundaries between adjacent diamond plates, the gaps between the adjacent diamond plates were totally filled up by CVD diamond. It is expected that a flat surface can be obtained by further optimization of the growth conditions and the basal mosaic arrangement.

4. Heteroepitaxial growth of diamond films on Pt(1 1 1)

The purpose of this subject is to deposit a grain-boundary-less diamond film on an area of 10 mm in diameter. Specifically, we are developing a heteroepitaxial growth technology of SCD film on Pt(1 1 1) whose diameter and thickness are 11 and 2 mm, respectively. This is based on the finding by Shintani [12] that a coalesced diamond film can be deposited on Pt(1 1 1), and we try to achieve a full coalescence over the entire surface of the substrate. Unlike HOD films on Si or SiC, the bias-enhanced nucleation is not necessary in this process. The standard polishing method is used to increase the nucleation density. Important factors for this

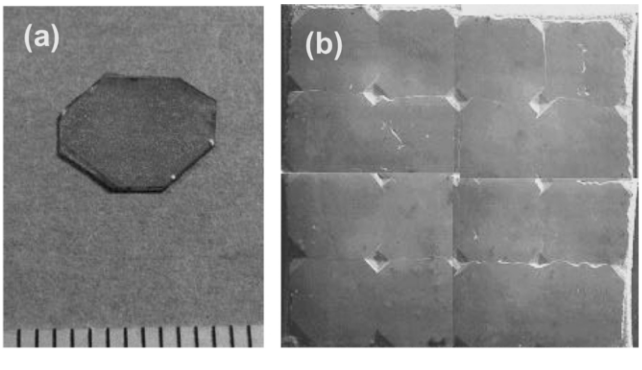

Fig. 5. (a) 8 mm single crystal of CVD diamond; and (b) 12×12 mm^2 size mosaic diamond of 1 mm thickness.

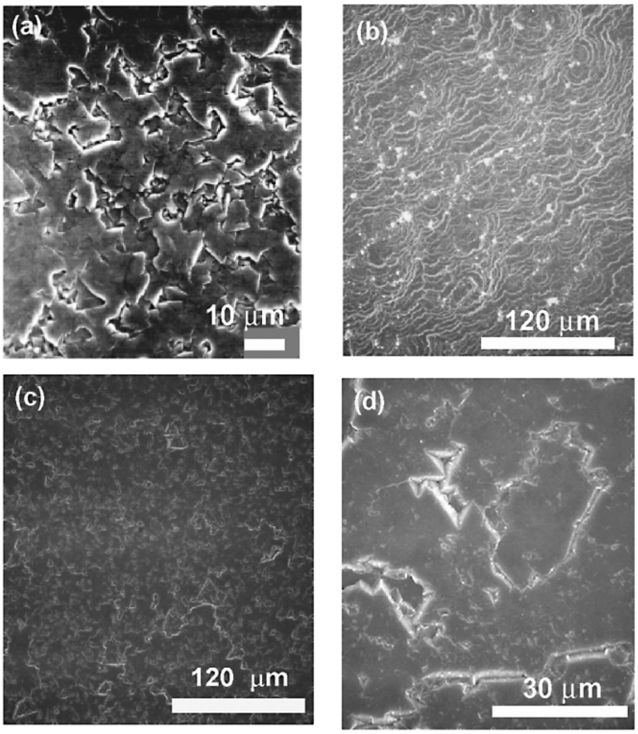

Fig. 6. (a) SCD film grown on Pt(1 1 1) [5]; (b) bunched steps on the peripheral regions; (c) SEM micrograph of B-doped film surface; and (d) a magnified view of (c).

technology are: (i) the crystal quality of Pt must be high, (ii) the orientations of nuclei must be best aligned by optimizing the initial growth conditions, and (iii) the lateral growth conditions in the final stage must be optimized. For experimental details, see Ref. [5].

Fig. 6a shows a surface morphology of SCD film grown under standard conditions. Fig. 6b shows the surface morphology in the peripheral area of the film deposited for 100 h. It is seen that the surface is covered with bunched steps, and no grain boundaries are seen. It was only 25–30% of the substrate surface that was covered by the morphology, and otherwise the film morphology was like the one shown in Fig. 6a. It has been known that (1 1 1) faces of diamond tend to appear if the diamond film is doped with boron (B). Thus, we deposited B-doped diamond on Pt(1 1 1) by adding B_2H_6 in the source gas. As a result of 100-h growth, a well-coalesced, ⟨1 1 1⟩-oriented diamond film was grown, demonstrating that the coalescence was accelerated between adjacent diamond (1 1 1) faces, as seen in Fig. 6c and d. Experiments are ongoing to further optimize various experimental conditions to achieve flatter film surfaces.

5. Microfabrication of diamond surface [6,7]

Fabrication technologies of a sharp tip and its array at (1 0 0) surfaces of single crystal diamonds is being developed using a combination of RIE, anisotropic growth of diamond by MPCVD, and microwave etching using CO_2+H_2. Such structures are expected to be used, for instance, for field emission tips, sensors and devices using vacuum microelectronics, actuators, and optical components. For such applications, a use of single crystal diamonds is advantageous over polycrystalline diamond films, because arrays of sharp tips with a regular shape can be fabricated uniformly, and the technique of anisotropic growth can be utilized.

In the RIE technique, a 13.56 MHz radio frequency (RF) plasma generation system was used. Usually, O_2 is used for diamond etching, but we found that an addition of 1–2 vol.% CF_4 to O_2 gives marked effects on etching. The total gas pressure used was 2–5 Pa, and the input RF power was 200 W. For microfabrication, circular Al masks were photolithographically fabricated on (1 0 0) diamond surfaces prior to the RIE. Consequently, an array of cylindrical columns were made, as shown in Fig. 7a. The length of the diamond column was 9.5 μm, and its diameter was 1.2 μm, i.e. the aspect ratio is 8. The etching rate was remarkably high, 9.5 μm/h. In certain cases, very thin columnar structures with a diameter of 0.2 μm and a length of 7.5 μm were formed among the cylindrical array, presumably because residual Al particles became micromasks. It is remarkable that the basal etched surface was very smooth: indeed, its roughness was smaller than the initial diamond surface. We infer that the formation of both the cylindrical structures with high aspect ratios and the smooth basal surface arise from a deposition of fluorinated carbon films that protect irregular etching. Also, we established a method to sharpen the top of each diamond cylinder of Fig. 7a using Al masks with nonuniform thickness in which the central region is thicker than the peripheral area. As the plasma etching proceeds, the Al masks also are gradually etched from the peripheral to the central areas, and hence a sharp needle shape is formed. As a result, a needle with a 2-nm top radius was fabricated.

Two other methods of fabricating protuberance on diamond surfaces have been developed. The first method is to start with a cylindrical column and undertake diamond CVD under proper conditions. This result is shown in Fig. 7b. The second method also starts with cylindrical columns of diamond shown in Fig. 7a, but followed by microwave etching using CO_2+H_2. As a consequence, we could fabricate a variety of shapes, from columns to protruded crystals as well as their combinations at (1 0 0), (1 1 0) and (1 1 1) surfaces of single crystal diamonds. This technique will be useful for fabricating diamond electron emitters, for instance, and currently emission measurements are ongoing.

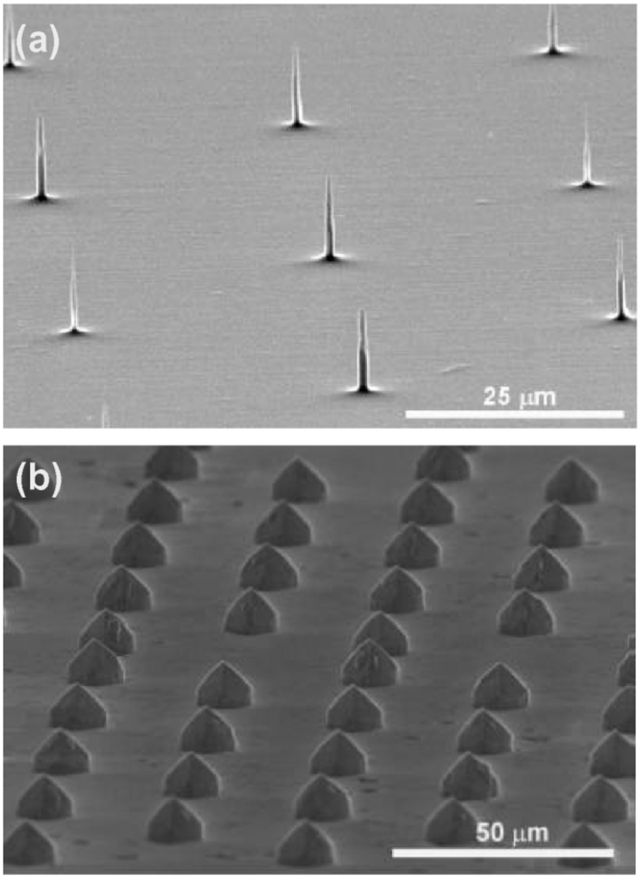

Fig. 7. (a) Array of cylindrical columns fabricated at single crystal diamond (1 0 0) surface; and (b) array of crystals fabricated by growing diamond on cylindrical columns.

6. Field emission from diamond

6.1. Temperature dependence

We are studying temperature dependence of field emission from diamonds with H- and O-terminated surfaces to see if there are any differences between them. In the present study, B-doped diamond layer was deposited on two type-Ib diamonds with (1 0 0) surfaces of 3 mm^2. For the diamond CVD, 0.5% $CH_4/H_2 + 6.25$ ppm B_2H_6 was used as the source gas, and the film thickness was estimated to be approximately 1 μm. After CVD, both specimens were cleaned using chromic acid and aqua regia, and one specimen was treated by hydrogen plasma at 60 Torr for 5 min. The filed emission measurements were carried out using a system described elsewhere [13]. The anode is a gold ball with a diameter of 2 mm, movable by a piezoelectric device, and the distance between the anode and the specimen was 1.5 μm.

The results of measurements are shown in Fig. 8a and b for H- and O-terminated specimens, respectively. It is seen that the temperature dependence are significantly different between the two. For the O-terminated specimen (Fig. 8b), the field emission current first decreased when the temperature T was increased from 20 to 70 °C, then increased when T was further raised to 170 °C. By contrast, for the H-terminated specimen (Fig. 8a), the field emission current increased monotonically as T was raised from 20 to 170 °C. This demonstrates that the field emission current is strongly dependent on how diamond surface is terminated. It should, however, be noted that in a separate series of experiments using B-doped polycrystalline diamond films, in which the B_2H_6 concentrations were 1 and 10 ppm, the field emission current of H-terminated diamond film decreased with increased T. We thus conclude that the field emission current is influenced by both orientation of the crystal facet and the B-doping concentration in addition to the surface termination.

6.2. High field emission current from ion implanted homoepitaxial diamond

It appears to be widely accepted so far that the field emission from diamond is most efficient if the diamond

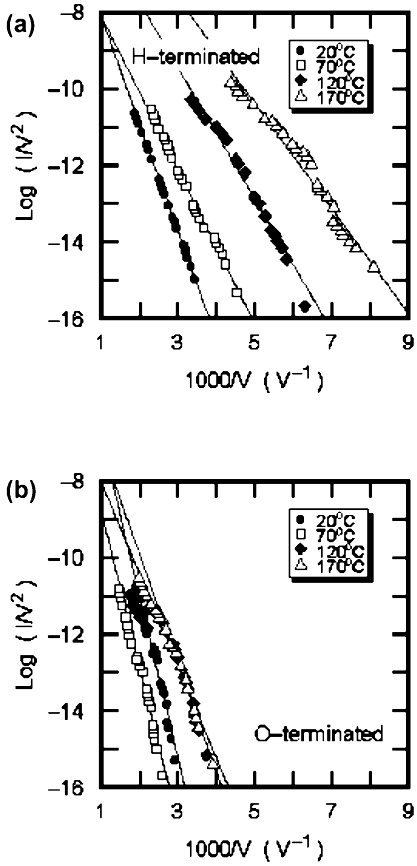

Fig. 8. Temperature dependence of field emission. (a) Fowler–Nordheim (F–N) plot for H-terminated single crystal diamond (1 0 0); and (b) F–N plot for O-terminated specimen.

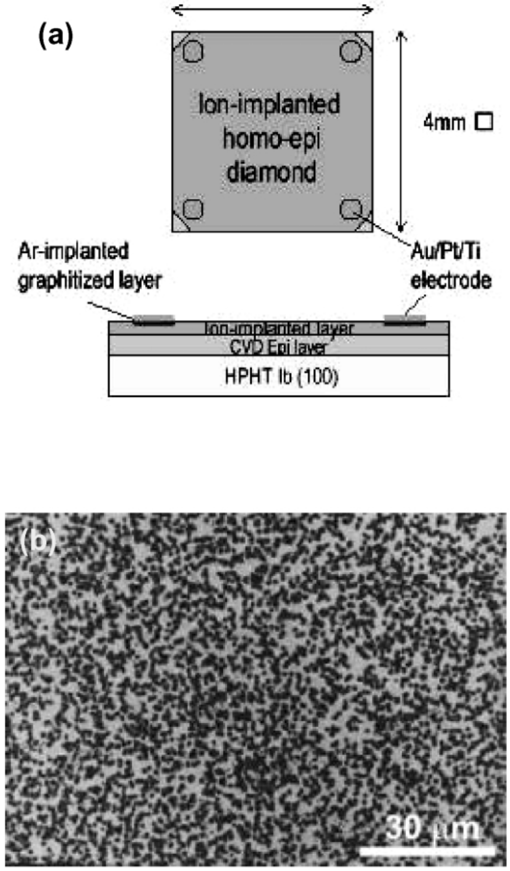

Fig. 9. (a) Device structure using single crystal diamond; and (b) P-implanted surface observed by SEM after electron field emission.

film is microcrystalline, containing a high density of grain boundaries and graphitic components. In the present study, we deposited a high quality homoepitaxial diamond layer on a type-Ib diamond (1 0 0) surface, ion implanted P, B or S, and measured the field emission from the specimen thus made. As a result, an emission current density of approximately 1.5 A/cm^2 was achieved from the area of approximately 0.07 mm^2 that had been P implanted [8].

Fig. 9a shows a schematic structure of the specimen. An undoped diamond layer with a thickness of 2–6 μm was deposited by MPCVD using 1 vol.% CH_4/H_2 under conditions of ($P_m = 4$ kW, $P = 100–110$ Torr, and $T_s = 850–900$ °C). The growth rate was approximately 3 μm/h. A cathodoluminescence measurement of this specimen exhibited an intense free exciton band at 235 nm at room temperature, indicating that the film quality was very high. To fabricate ohmic electrodes in the four corners of the specimen, Ar ion was implanted to $10^{16}/cm^2$ to make the surface graphitic, which was then followed by a deposition of Au/Pt/Ti electrodes by electron beam deposition. As a result, a contact resistance of 10^{-7} Ω cm was achieved. Finally, multiple ion implantation of P, B or S was done to achieve an atomic density of $10^{20}/cm^3$ in diamond at the maximum. Fig. 9b shows a SEM of the specimen surface (after the field emission measurements) implanted with P. It is seen that dark spots, which are actually vertical lines, were formed by ion implantation.

For the measurement of field emission current, a rod of W–Re alloy with a diameter of 300 μm was placed 28 μm above the center of the specimen. The applied voltage was 4 kV at the maximum. It was found that the emission current is correlated with the conductivity of the implanted diamond layer, and a maximum current of 1.5 A/cm^2 was observed for a P-implanted specimen. It is inferred that electrons are supplied from the ohmic contacts at the corners, travel along the implanted layer, and come up to the surface through the vertical channels formed by ion implantation. Since diamond is so hard and has such a high thermal conductivity, the specimen was able to resist the heat generated by the channel conduction of electrons, and sustain such a high current density.

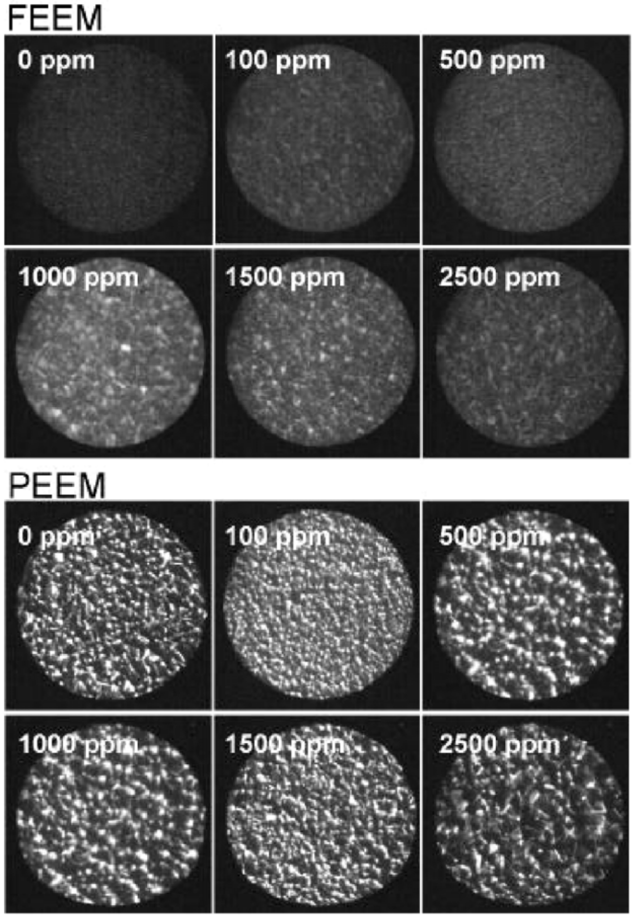

Fig. 10. FEEM and PEEM images of polycrystalline diamond films with different B concentrations. The number in each figure stands for B/C, the atomic B concentration against the C concentration in the source gas, for CVD. The window is 50 μm in diameter.

6.3. PEEM and FEEM measurements [14,15]

Both PEEM and FEEM are very useful tool to identify the location of electron emission. Such measurements have been done at North Carolina State University for a variety of specimens that the FCT Project had made. One example is PEEM and FEEM measurements of B-doped diamond films grown on p-Si(1 0 0) substrates. The films were synthesized using a quartz-tube-type MPCVD reactor for 12 h for atomic B/C ratio in the source gas below 2500 ppm. The observed results are shown in Fig. 10. We had anticipated that the field emission intensity changes monotonously with B-doping concentration. Unlike such an assumption, the observed results showed that for FEEM, the intensity was maximum when B/C = 1000 ppm, as seen in Fig. 10. Unlike the results of FEEM, PEEM data showed no distinction between specimens with different B concentrations. One may notice that PEEM images somewhat reproduce the original film morphology, as electrons tend to be emitted from the top and edge areas of each grain more than lower regions such as grain boundaries. It has not yet been understood why the 1000-ppm B-doped specimen emits electrons more than others, but it is inferred that the specimen has an optimized film resistivity and surface roughness.

7. Conclusions

For practical applications of diamond films, (i) development of production scale reactors with precise process control and (ii) large single crystal synthesis by homo- and heteroepitaxy are most important at the present stage along with feasibility studies of device and other applications. It is our expectation that the technologies and international collaborations established during the FCT Project will give useful contributions for diamond research in the coming generations.

Acknowledgments

Our activities have been strongly supported by Prof. M. Yoshikawa, Dr H. Okushi, Prof. H. Kawarada, Dr S. Fujiwara, and Dr Y. Koga as well as FCT staff members. We would like to thank all of them for continuous encouragement. This work was supported by Japan Fine Ceramics Center (JFCC) that was consigned by New Energy and Industrial Technology Development Organization (NEDO).

References

[1] E. Sevillano, in: B. Dischler, C. Wild (Eds.), Low Pressure Synthetic Diamond, Springer, 1998, p. 11.
[2] T. Tachibana, Y. Ando, A. Watanabe, et al., Diam. Relat. Mater. 10 (2001) 1569.
[3] Y. Ando, Y. Yokota, T. Tachibana, et al., Diam. Relat. Mater. 11 (2002) 596.
[4] K. Meguro, T. Matsuura, T. Imai, Diam. Relat. Mater., submitted for publication.
[5] T. Tachibana, Y. Yokota, K. Miyata, et al., Phys. Rev. B 56 (1997) 15967.
[6] Y. Nishibayashi, H. Saito, T. Imai, N. Fujimori, Diam. Relat. Mater. 9 (2000) 290.
[7] Y. Nishibayashi, Y. Ando, H. Saito, T. Imai, T. Hirao, K. Oura, Diam. Relat. Mater. 10 (2001) 1732.
[8] T. Sakai, H. Sakuma, M. Suzuki, T. Ono, H. Yoshida, Proceedings of the Fifteenth New Diamond Symposium, New Diamond Forum, pp. 200 (in Japanese).
[9] C. Wild, R. Kohl, N. Herres, W. Müller-Sebert, P. Koidl, Diam. Relat. Mater. 3 (1994) 373.
[10] G. Janssen, L.J. Giling, Diam. Relat. Mater. 4 (1995) 1025.
[11] C. Findeling-Dufour, A. Gicquel, Thin Solid Films 308–309 (1997) 178.
[12] Y. Shintani, J. Mater. Res. 11 (1996) 2955.
[13] Y. Gotoh, T. Kondo, M. Nagao, et al., J. Vac. Sci. Technol. B 18 (2000) 1018.
[14] F.A.M. Kock, J.M. Garguilo, B. Brown, R.J. Nemanich, Mater. Res. Soc. Symp. Proc. 621 (2000) R651.
[15] F.A.M. Köck, J.M. Garguilo, R.J. Nemanich, Diam. Relat. Mater. 10 (2001) 1714.